Using Object-Based Image Analysis approach for analyzing the impact of annual average change of climate elements on LULC change in northern of Sulaimani province

Mohammed W. Mohammed [1], Salam M. Nasir[2] and Sarkar H Khdir[3]

[1] Department of Geography, college of Humanities, University of Raparin-Rania, Kurdistan Region, Iraq
[2] Department of Remote Sensing and GIS, University of Tabriz, Tabriz, Iran
[3] Department of Geoinformatics (Z-GIS), University of Salzburg, Salzburg, Austria

ABSTRACT

Environmental resources are critical to the long-term development and provision of human needs; nonetheless, they continue to be threatened by negative changes as a result of human and natural challenges. One of the most pressing issues the world has faced today is climate change; this phenomenon has had severe impact on the natural environment and the whole ecosystem. It is thought to be the most essential determinant in land use/ land cover (LULC) change. However, LULC changes are important components of contemporary environmental monitoring and management systems, as well as a large and crucial element of research to emphasize the regional, local, and global climate change effects.

This research's interest is on the Northern parts of Sulaimani province, in Iraq's Kurdistan Region, is located between longitudes (44° 33' 40.6" - 45° 23' 9.98") east and latitudes (35° 35' 11.45" - 36° 30' 6.28") north in the region's northern and north-eastern parts. It covers an area of 4012.92 square kilometers and is divided into three districts (Rania, Pshdar, and Dukan). The northern of Sulaimani, like any other regional and global area, is not immune to the effects of global warming and climate change, including annual droughts and climate fluctuations, the consequences of which are clearly seen in LULC change, especially in the change of vegetation cover, and the area of water bodies, as well as the cultivation patterns of the study area.

KEY WORDS: Climate change, LULC change, RS& GIS, Northern of Sulaimani, OBIA.

1. INTRODUCTION

Large parts of the world are currently undergoing significant land use/cover (LULC) changes which are causing environmental, social, and economic challenges (Lamichhane, S. et al, 2019). Climate change and LULC changes are two major global ecological concerns that will have an impact on a significant percentage of the earth's crust in the future. The causes and consequences of human-caused climate change and land-use activities have mostly been studied independently until now. Climate change and LULC change, on the other hand, are interconnected (Dale, V. H. 1997). LULC change, which corresponds to the alteration or exchange of cover types, is a measure of major natural and anthropogenic ecological disturbance. It's crucial in the global changing process, especially when it comes to climate systems (Fasona, M. J. et al. 2014). On the other hand, the current climate's general increase in temperatures and decrease in rainfall are expected to have detrimental effects on land-cover. This raised the possibility that climate change will become a major driver of future ecological changes and biodiversity (Leary, N. et al. 2007). Generally, Changes in land use and land cover (LULC) are essential indicators of global ecological and environmental change, as well as a key component of comprehending human-natural system interactions (Chen, H. et al, 2018). LULC Change is triggered by a number of factors, many of which can be traced back to human activity, such as population growth, economic development, and globalization; it is also influenced by natural processes such as floods, landslides, droughts,

and climate change, though it is influenced to some extent by anthropogenic activity (Näschen, K. et al, 2019).

The term "global warming" refers to an increase in the Earth's average temperature. As the Earth warms, natural calamities such as storms, droughts, and floods become more common (Venkataramanan, M. (2011)). Changes in the lithosphere, hydrosphere, biosphere, and atmosphere, have sparked concern about the potential consequences of global warming (Aggarwal, S. P. et al. 2012). Although, one of the main causes of long-term global warming is inappropriate use of natural resources and changes in land use in general. However, as one of the repercussions of climate change and global warming, changes in average annual climate factors may have an impact on current and long-term effects on LULC change (Diener, B. J., & Frank, W. P. 2010); As a result, we may conclude that climate change and land use change are linked in two ways. Therefore, understanding the effects of climate change is critical for forecasting future LULC and land management needs and vice versa (Li, C., Li, Z, et al. 2021). The northern part of Sulaimani in Iraq's Kurdistan Region, like any other regional or global area, is vulnerable to the effects of global warming and climate change, including annual drought and climate fluctuations. As we have seen in the past year, the area has experienced severe drought, the consequences of which are clearly visible in the change of LULC.

There are two methods for capturing LULC dynamics: traditional ground-based methods and remote sensing-based methods. The first method is very labour intensive, time consuming, and difficult to capture data (Idowu, T. E. et al, 2020). Remote sensing and GIS techniques, on the other hand, are regarded as the most effective and efficient technologies for LULC changes (Goodin, D. G. et al, 2015). There are several techniques for extracting meaningful information about LULCs from remotely captured datasets. Object-based image analysis has recently become more popular for remote sensing image categorization (DeWitt, J. D. ET AL, 2017). OBIA classification classifies groups of pixels based on their spatial connection to neighbour pixels and the relevant properties of those pixels. The pixel-based approach is based on the spectral characteristics of single pixels, whereas polygons are the building blocks of the object-based image analysis (OBIA). Polygons, also known as image objects, are groups of pixels that share common characteristics such as spectral signatures and contexts (Son, N. T. et al, 2014; Ma, L. et al, 2019). Finally, the primary goal of this study is to integrate and use several datasets from remote sensing (RS) and geographic information systems (GIS) methodologies to assess the impact of climate change on LULC change patterns in northern Sulaimani from 2013 to 2021, using Landsat sensor data (OLI) and object-based image analysis (OBIA).

2-Study Area:

The northern of Sulaimani province is a part the Kurdistan Region of Iraq, which is situated between longitude (44° 33' 40.6" - 45° 23' 9.98") east and latitude (35° 35' 11.45" - 36° 30' 6.28") north. It consists of the three districts (Rania, Pshdar, and Dukan), and has an area of (4012.92) square kilometers (Figure1). The study area is enriched with water resources, deferent climates, as well as differences in topography between the southern and northern parts, which reflect the region's natural resources. The Mediterranean climatic system has a strong influence on the study area. The hot and dry summer season, with an average temperature of (35.6°C), and the average temperature throughout the cold and rainy winter was (7.7 °C), while the annual average precipitation is about 622.2 mm/year (General directorate of meteorology and earthquake of KRG 2019). The northern of Sulaimani, like any other regional and global area, is not immune to the effects of global warming and climate change, including droughts and climate fluctuations, the consequences of which are clearly seen in the change of LULC, especially in the change of vegetation cover, and water bodies, as well as the cultivation patterns of the study area.

In terms of water resources, Dukan lake is located in the middle of the study area, which has an area of about 278.52 km2, and there is a main river in the area known as lesser Zab. In terms of topography, the study area consists of a series of high and complex mountains, plains, valleys, and hills. The most famous mountains of the area are (Asos, Kewarash, Makok, Mamanda, and Qandil) with an average height of (1734) meters above sea level, the maximum point is (3112) meters, and the minimum point is (357) meters above sea level (Sulaymaniyah Statistical directorate, 2020). It also has very fertile plains such as (Pshdar, Bitwen, Marga, and Piramagrwn) (Figure2).

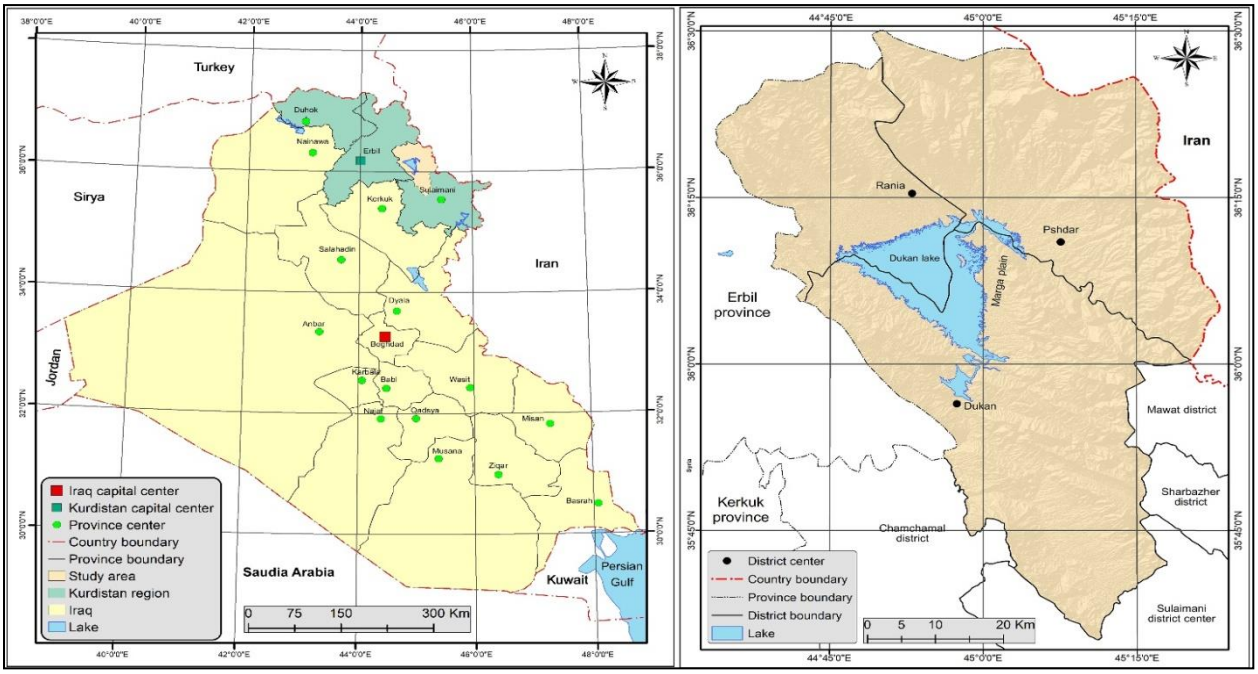

Figure 1: Location of study area.

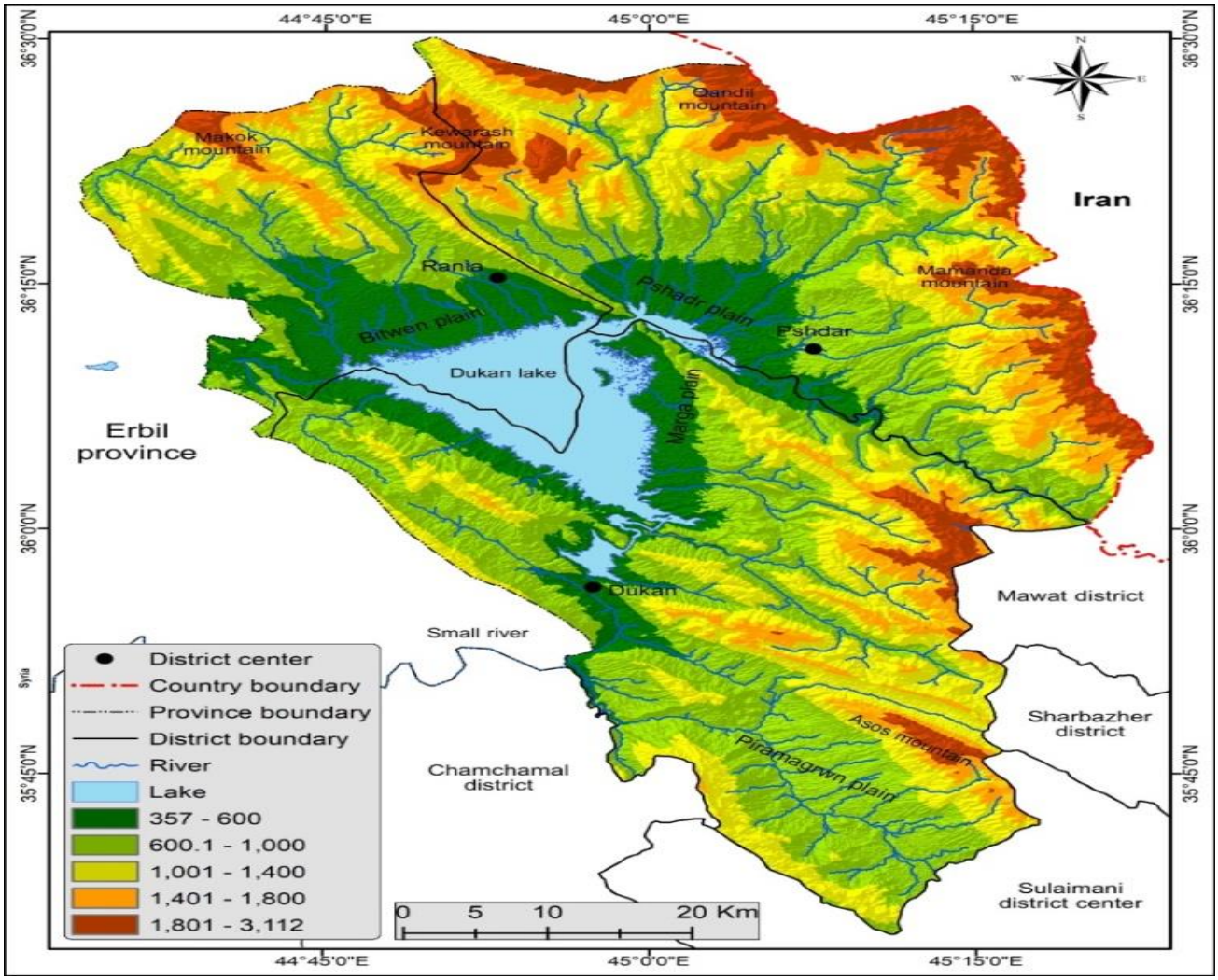

Figure 2: Topography and water resources in the study area.

3-Material and Methods:

The research methodology has taken the following procedures as shown in figure (3), in order to get reliable and accurate results, as well as to achieve the main goal of the study.

3-1 Datasets and preparation:

In this study we have used various types of data. They were taken from different sources, as shown in Table (1). 9 raw satellite images with 15-m spatial resolution (Landsat8 Oli) (after Gram-Schmidt Pan sharpening) for July 2013 to 2021 were used to obtain the LULC map. A digital elevation model (DEM) with a spatial resolution of 15 m was also used, and a set of secondary variables were generated from the above data, including NDVI, NDBI, and NDWI images, as well as elevation and slope maps, which were used as an effective adjunct to the OBIA process. In addition, several statistical data sets such as hydrology and meteorology were employed to investigate the relationship between LULC Change and average climatic values in the study area.

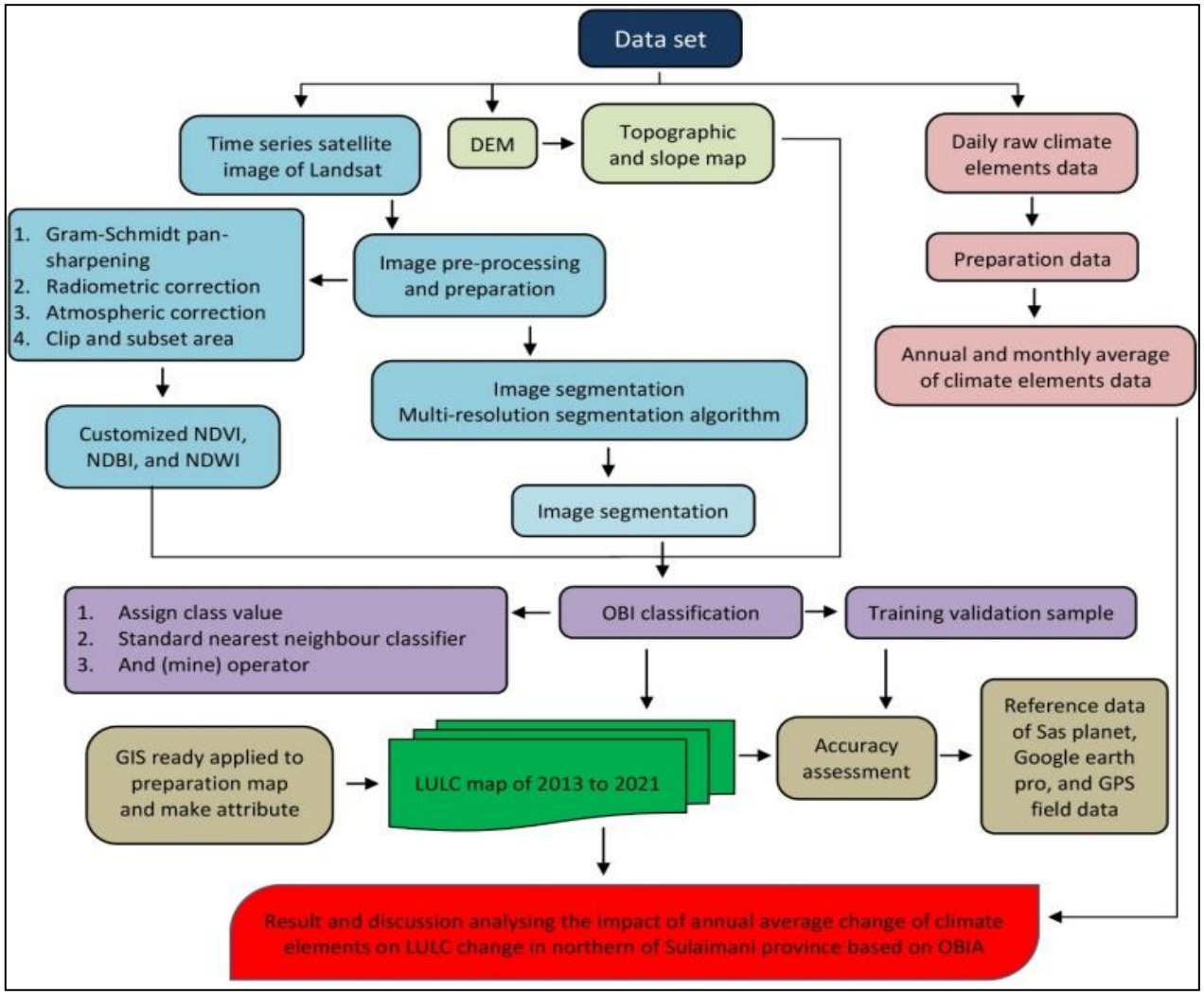

Figure 3: Research methodology process

Table 1. Summary of spatial datasets used in this study.

Data	Types of data	Acquisition Date (s)	Spatial Resolution/ Scale	Data Sources
Landsat 8 Oli	Raster	17072013, 20072014, 07072015, 09072016, 12072017, 31072018, 18072019, 04072020, 07072021	15 m	https://earthexplorer.usgs.gov
Aster DEM	Raster		15 m	
Topographic Map	Raster		15 m	Derived from DEM
Slope Degree	Raster		15 m	Derived from DEM
Boundary of the Study Area	Vector	2021		Ministry of Transport, Sulaymaniyah Statistics Directorate, GIS Department
Meteorology	Primary	2013 - 2021		Ministry of Transport, Dukan Weather Station

In order to prepare the data for image processing (OBIA) and analysis of the link between LULC change and annual average change of climate factors in the study area, numerous pre-processing steps were done on all of the images utilized in this study. Although, the satellite images all have the same spatial resolution (30 m) and sensor (Landsat8 Oli), but the spatial resolution of the multi-spectral bands has been enhanced to 15 m by implementing the Gram-Schmidt Pan Sharpening (GSPS) technique and using the panchromatic band. Additionally, each image was radio-metrically corrected by converting raw digital numbers (DNs) to top of atmosphere (TOA) reflectance values to account for changing sun angles and surface reflectance variations, as well as using an atmospheric correction approach to reduce atmospheric effective. Finally, all of the images for each phase were clipped to the study area. Moreover, various indexes, such as NDVI, NDBI, and NDWI, were customized in this study using the equation (1,2,3), and these indices are commonly used to separate some specific categories (Bhatti, S. S., &Tripathi, N. K. 2014; Talukdar, S. et al, 202; Ali, M. I. et al, 2019).

[1]NDVI = (NIR– RED) / (NIR + RED)
[2] NDBI = (NIR – SWIR) / (NIR – SWIR)
[3]NDWI = (GREEN – NIR) / (GREEN + NIR)

Also, several raw meteorological datasets, including daily precipitation data, temperature and humidity were gathered from official institutions in order to investigate and quantify the association between annual average change of climate elements and LULC change in the study area.

3-2 Image segmentation:

Image segmentation is the first step in most OBIA procedures, and it involves grouping pixels into image objects (Feizizadeh, B, et al. 2021), also it involves dividing an image into sections that are relatively homogeneous and utilizing the segments' spectral, spatial, and contextual features in order to achieve the best results for various categories (Johnson, B. A., & Ma, L. 2020; Ming, D. et al, 2015). Segmentation parameters and algorithms have a direct impact on the size and kind of image objects (Georganos, S. et al, 2018). There are numerous techniques and algorithms for image segmentation available. The multi-resolution segmentation algorithm was chosen for the image segmentation process in this study, as it is an efficient and commonly used segmentation approach in OBIA (Tian, J., & Chen, D. M. 2007). However, to develop the most appropriate and final scale parameter, several scale parameters were analyzed and assessed before determining the most acceptable scale in this study. The segmentation was done on two scales (50 and 70), both of which had the same form factor (0.6) and compactness factor (0.4).

Applied Object based image classification and LULC mapping:

The 9 LULC classes were created and developed the LULC maps using satellite images by object-based image analysis methods for nine phases between 2013 and 2021.This is accomplished with the

application of a novel effective technique known as Assign Class, which also separates the required categories utilizing spatial, spectral, and textual information from the objects (table 2). In addition, a standard nearest neighbor classifier with (min) operator was employed to classify the data in the eCognition Developer 9.0 software. The study area is separated into two components in the first step of the classification process: water body and land area. In the second step, Land areas are split into sub-zones depending on relief and slope values, such as mountainous areas, plain areas, and other areas. Each of these sub-zones was then reclassified, and the study's primary classes were split based on distinctions in spatial, spectral, and textural properties. For example, in high mountainous areas, snow areas, dense grass, moderate to poor grass, and bare land are separated, while in plain areas, agricultural use, dense grass, moderate to poor grass, Built-Up, and bare lands are separated. Finally, other areas classes such as forest area mixed with dense grass, moderate to poor grass, Built-Up, and bare lands are classified.

Furthermore, to confirm the correctness of the results acquired, a full inspection of the produced results has been made feasible, as shown in Figure (4), by visiting the field and checking various values of items. All sub-classes with the same names in the study area's sub-zones are merged. Finally, after determining the effect of the assigned class values used to separate the specified classes, all of the classified classes are exported as vector files, and the GIS ready technique is implemented in Arc Map GIS 10.8 to build LULC maps for all stages and generated attribute tables.

Table 2: Description of LULC categories and assign class values to separate them.

LULC Categories	Description	assign class values
dense grass	The natural vegetation in the highlands and all other areas are covered with dense grass.	Mean DEM >= 1800 and Mean DEM <= 3107 > 1800/ Area of > 1800 with NDVI >= 0.2/ NDVI >= 0.13 and NDVI < 0.142/
moderate to poor grass	An area that is moderately or very little covered with natural vegetation.	> 1800 with NDVI >= 0.15 and NDVI < 0.2/ NDVI >= 0.11 and NDVI < 0.13/ > 1800 with NDVI >= 0.05 and NDVI < 0.15/ NDVI >= 0.05 and NDVI < 0.11/
forest area mixed with rangeland	All areas are covered with dense, temperate, and open forests, as well as shrub lands mixed with dense pastures.	unclassified with NDVI >= 0.25/ unclassified with NDVI >= 0.142 and NDVI < 0.25
irrigated agriculture	All farms that use irrigation to grow summer crops such as tomatoes, cucumbers, watermelons, melon, and a variety of other fruits and vegetables.	Mean Slope < 6.8 and Mean Slope >= 0 / NDVI >= 0.19
harvested ad cultivated farms	Cereal, particularly wheat and barley, is harvested on farms that rely on rain for irrigation during the wet season. Furthermore, all farms are cultivated, as are abandoned fields.	Mean B1 >= 11690 and NDVI < 0.19/ Mean B1 < 11690 and NDVI < 0.19 /
water body	It has a number of permanent rivers, lakes, dams, and fish ponds.	Ratio B1 >= 0.204 and NDVI < 0.027/ Ratio B1 >= 0.204 and Mean DEM < 450/ NDWI>=0.142
snow area	High mountain areas covered with snow.	Area of > 1800 with Brightness >= 17000 and Mean DEM >= 2110
bare lands	Lands without vegetation cover as a result of arid, riverbeds, soil erosion, scorched areas, and barren rocky areas.	Ratio B1 >= 0.195 and NDVI < 0.1/ NDVI < 0.05 /> 1800 with NDVI < 0.05/ Brightness≥17000/ mean slope >= 45
Built-up	Residential areas include city and town area.	NDBI> –0.033, NDBI<0.26/ mean B1 > 12690 NDVI<0.18/ 0.125<Asymmetry<0.876

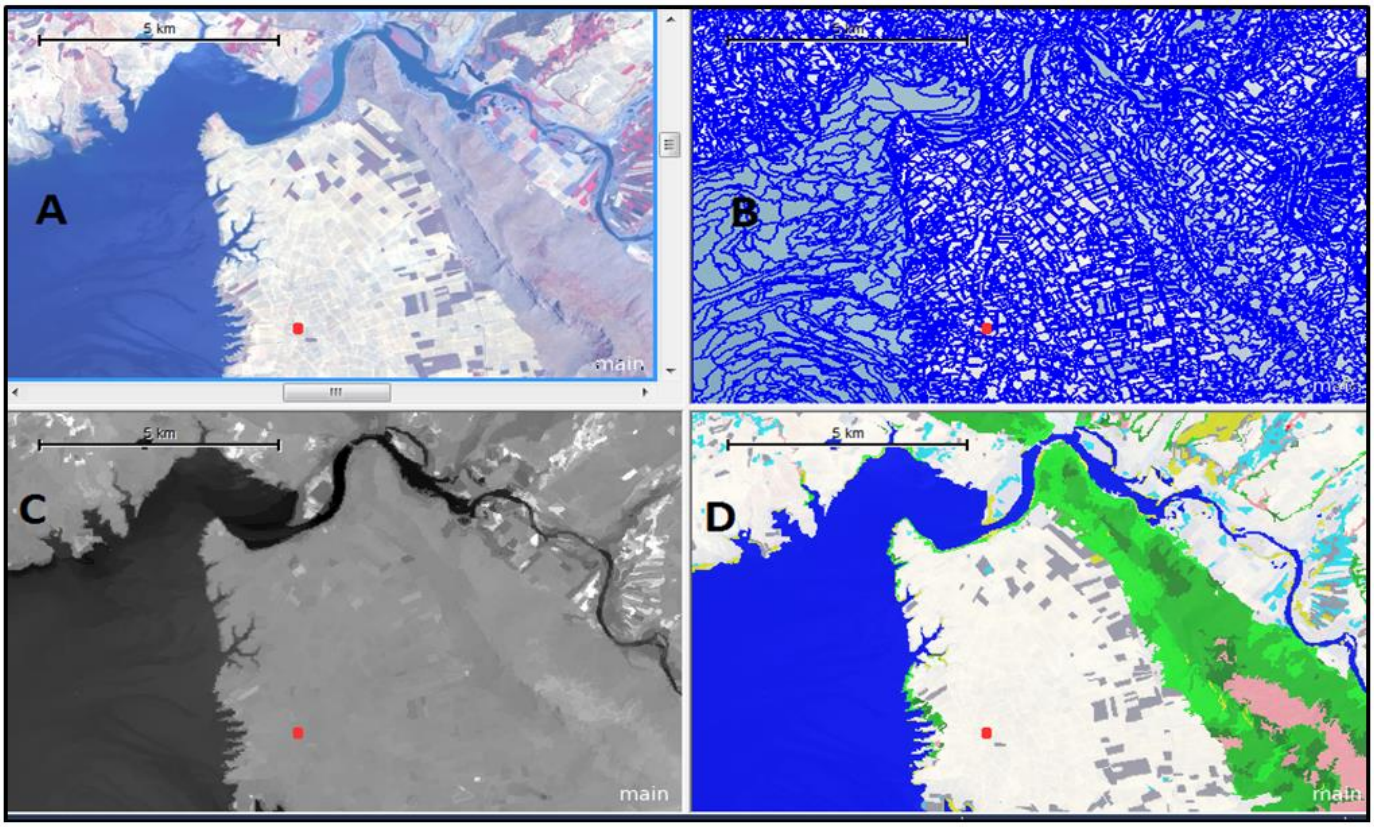

Figure 4: A zoomed part of the study area A) false color band image B) Image segmented C) image with NDVI feature value, and D) result of OBI classification.

3-3 Accuracy Assessment of LULC Maps:

Any categorization procedure must include an accuracy assessment (Hossen, S. et al, 2019). It compares the categorized image to data from another source that is thought to be accurate or ground truth (Thakur, T. K. et al, 2020). The evaluation can be done in two ways: qualitatively or quantitatively (Dong, S. et al, 2020). The goal of accuracy assessment is to evaluate how well ground objects are mapped in terms of their shape, size, and position (Ye, S. et al, 2018) as well as to estimate the error and uncertainty of the output classification in order to either choose the most appropriate mapping procedure or to inform interpretation of the output (Lyons, M. et al, 2018). The accuracy assessment of LULC maps created from remotely sensed data is critical because it provides map users with data quality information. Confusion matrix is a widely used technique for calculating a number of accuracy measures. (Dharani, M., &Sreenivasulu, G. 2021: Twisa, S., &Buchroithner, M. F. 2019).

After generating the classified images in this study, the stratified random technique was used to assess the accuracy of LULC maps derived from satellite imagery, with each of nine LULC maps representing the different LULC classes in the study area. The accuracy was determined by employing (80 to 100) Validation points per class and was based on the use of Google Earth Pro, SAS Planet open source, visual interpretation, and ground truth data gathered by GPS in the field. In this study, the overall accuracy (OA), kappa coefficient (KC), Producer Accuracy (PA), and User Accuracy (UA) of classified maps are calculated using the error matrices technique, according to the equations below (Vivekananda, G. N. et al, 2021):

$$Producer's accuracy(\%) = \left(\frac{x_{kk}}{x_{+k}}\right) X100 \quad (1)$$

$$User's accuracy = \left(\frac{x_{kk}}{x_{k+}}\right) X100\% \quad (2)$$

$$\text{Overallaccuracy(OA)} = \frac{1}{N}\sum_{k=1}^{r} n_i \quad (3)$$

$$\text{Kappacoefficient(k)} = \frac{N\sum_{k=1}^{r} x_{kk} - \sum_{k=1}^{r}(x_{k+}\cdot x_{+k})}{N^2 - \sum_{k=1}^{r}(x_{k+}\cdot x_{+k})} \quad (4)$$

Where N represents the total number of pixels, r represents the number of classes, xkk represents the total pixels in row "k" and column "k," xk+ represents total samples in a row "k," and x+k represents the total samples in column "k" in the error matrix.

4-Results and discussion:

4-1 Annual average change of climate elements:

The average monthly and annual changes in the elements of climate in the study area, which include precipitation (Millimeter), temperature (Celsius), and humidity (percent), are presented in tables (3, 4, and 5) for all stages of the study. The total rainfall has varied greatly throughout the research, with the highest rainfall of 1038 mm recorded in the 2019 rainy season and the lowest rainfall of 351.6 mm reported in the 2021 rainy season. Other characteristics of the climate have altered normally in relation to the average annual change.

The table (3). Monthly and yearly rainfall (mm) averages in the study area.

No	2013	2014	2015	2016	2017	2018	2019	2020	2021	Average
October	7.8	0.4	84.5	70.2	1	8.6	30.6	57.6	0	29.0
November	73.6	87.4	136.5	207.7	1.4	21	100.5	28.4	59	79.5
December	116.8	57.9	94.6	62.4	222	34.2	287.2	67.6	41.2	109.3
January	129.8	58.6	59.7	89.2	48.2	65.6	160.8	87	62	84.5
February	162.7	0.2	35.8	108.8	77.8	325.2	105.8	135	82	114.8
March	17.1	146.4	123.4	243.4	120.8	30.2	158.6	129	67.6	115.2
April	25.1	45.3	45.3	122.8	48	72.8	175.1	37.8	22	66.0
May	18.9	8.8	6.6	5.2	5.6	87.6	19.8	17	7	19.6
June	0	0	0.4	1.2	0.2	0	0	4.8	0	0.7
July	0	0	0	0	0	0	0	0	0	0.0
August	0	0	0.4	0	0	0	0	0	10.8	1.2
September	0	0	20.5	0	0	0	0	0	0	2.3
Sum	551.8	405	607.7	910.9	525	645.2	1038	565	351.6	622.2

In 2021, the highest average temperature was 21.88degrees Celsius, while the lowest average temperature was only 19.8 degrees Celsius in 2019.As for the average humidity, it appears that the highest humidity rate was recorded in 2019 with (50.03%), as well as, the lowest humidity in 2021 with (39.99%). The table shows the variations in yearly and monthly elements across the study period.

The table (4). Monthly and yearly temperature (Celsius) averages in the study area.

No	2013	2014	2015	2016	2017	2018	2019	2020	2021	Average
October	24	22.5	22.1	22.9	24.3	23.1	24.5	24.1	25.5	23.7
November	16.4	15.9	13.4	13	15.3	15.3	4.6	15.7	16.6	14.0
December	9.8	8	9.6	8.3	7.7	11.8	10.1	10.9	10.5	9.6
January	7.5	8.4	7.5	6.5	7	8.9	7.5	7.6	8.1	7.7
February	9.8	9.6	9.6	10.6	12.4	10.4	9.1	7.4	9.9	9.9
March	13.2	13.9	12.9	13.1	12.4	16.1	10.5	14	14.1	13.4
April	19.1	17.8	17.3	18.4	17.6	18.9	14.5	18.5	18	17.8
May	24.7	25.7	25.9	25.3	25.1	23.5	24.4	25.6	25.8	25.1
June	31.6	31.8	32	31.5	31.6	31.9	32.8	31.5	31.7	31.8
July	35	35.3	36.2	35.5	36.2	35.9	34.1	36.5	35.4	35.6
August	34.6	35.2	35.9	36	36	34.8	35.2	34.3	36	35.3
September	29.4	30.2	30.9	29.8	31.9	31.3	30.3	32.9	31	30.9
Average	21.258	21.19	21.11	20.91	21.46	21.83	19.8	21.6	21.88	21.2

4-2 LULC Change:

In the study area, nine LULC types were extracted with different reference years, ranging from 2013 to 2021. (Figure 5, 6, and 7). At the start of the study period (2013), the dominant LULC type was moderate to poor grass, accounting for 32.1 % of the study area, followed by forest Area with range land (29.7 %), harvested and cultivated farms (21.3 %), dense grass (9.21 %), and water body (4.61 %) (Table 6). Irrigated agriculture, built-up areas, bare lands, and snow areas, made up a small proportion of the total area, accounting for 1.52 %, 1.14 %, 0.42 %, and 0.01 %, respectively. Despite the fact that the LULC area changed in 2014, they remain listed in the same order. During the other stages (2015 to 2020) of the study period, forest Area with range land was the dominant LULC type, with snow area accounting for a small proportion of the total area.

The table (5). Monthly and yearly Humidity (%) averages in the study area.

No	2013	2014	2015	2016	2017	2018	2019	2020	2021	Average
October	38	31	47.7	48.4	29.9	27.7	37.5	38.7	34.6	36
November	61.1	58	62.1	67.8	34.5	56.2	69.2	42.5	48.4	56
December	71.8	59.2	77.2	65.6	68	58.9	79.6	70.3	75.8	70
January	69.2	67.6	70.3	73.1	66.2	63.5	74.4	68.2	62.1	68
February	73.3	48.9	66.1	63.6	62.1	68.8	71.3	65.4	55.6	64
March	57.8	62.8	59.8	64.1	63.2	53.8	72.3	58.4	55.2	61
April	46.3	56.3	54.7	56.1	57.1	51.3	70.4	56.7	50	55
May	38.1	31.6	30.5	37	31.4	50.3	44.8	42.4	29.8	37
June	17.4	18.4	17.3	21.3	18.5	20.9	21.4	19.9	17.6	19
July	15.8	16.1	14.6	17.4	14.7	15.3	17.9	18.2	15.4	16
August	16.6	15	15.7	16.5	15.8	17.6	19.7	18.5	18.1	17
September	19.8	20.2	22.8	20.7	17.2	18.9	21.9	19.8	17.3	20
Average	43.767	40.43	44.9	45.97	39.88	41.93	50.03	43.3	39.99	43.3

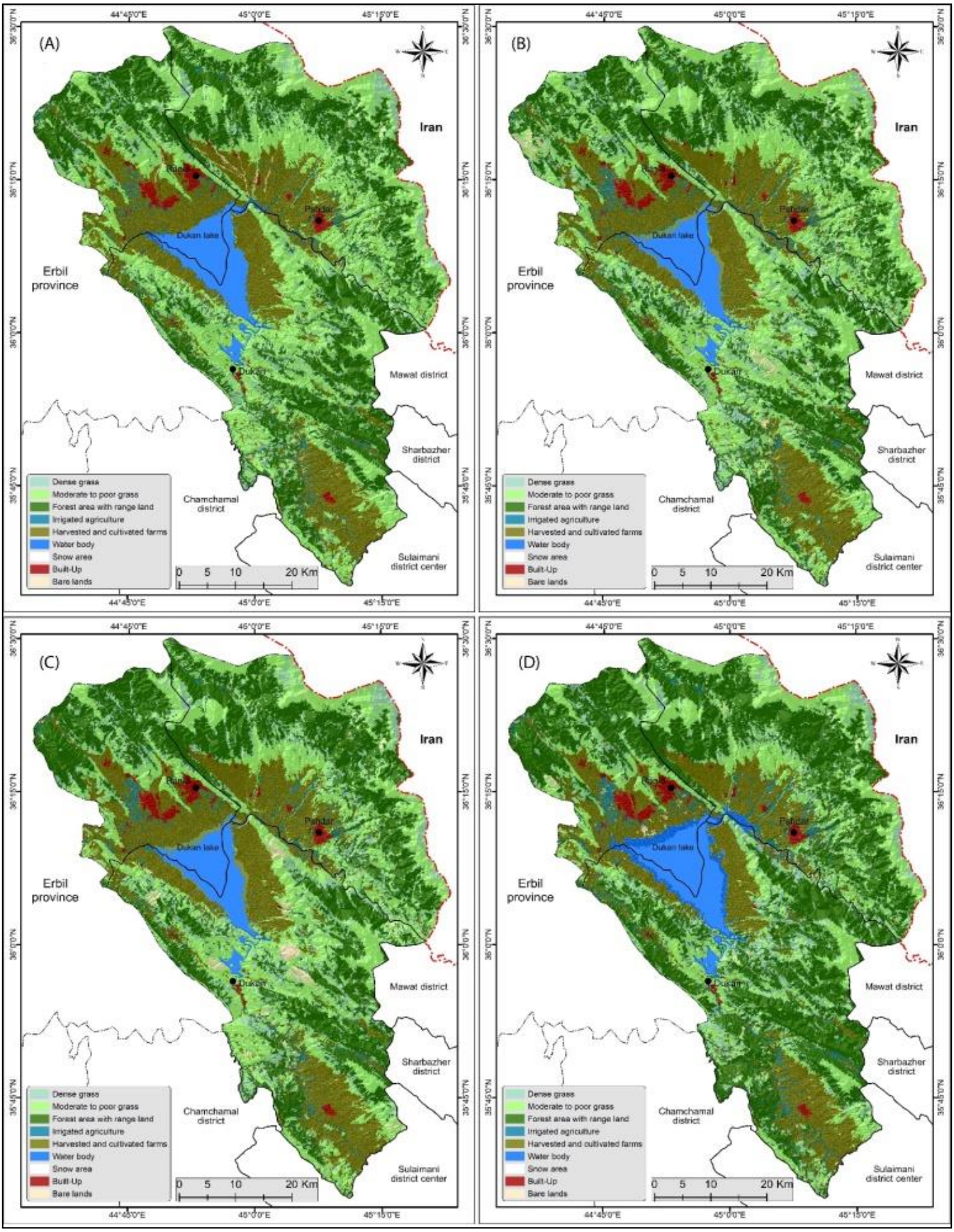
(A)
(B)
(C)
(D)
Iran
Erbil province
Dukan lake
Pshdar
Dukan
Mawat district
Sharbazher district
Chamchamal district
Sulaimani district center
Dense grass
Moderate to poor grass
Forest area with range land
Irrigated agriculture
Harvested and cultivated farms
Water body
Snow area
Built-Up
Bare lands
0 5 10 20 Km
44°45'0"E
45°0'0"E
45°15'0"E
36°30'0"N
36°15'0"N
36°0'0"N
35°45'0"N

Figure (5); OBI classification results: A) 2013, B) 2014, C) 2015, and D) 2016

However, the dominant LULC type at the end of the study period (2021) was forest Area with range land, accounting for 37 % of the study area, followed by moderate to poor grass (25 %), harvested and cultivated farms (20%), dense grass (8.5 %), and water body (4.5 %). Irrigated agriculture, built-up areas, bare lands and snow areas each accounted for a small percentage of the total area, accounting for 1.9 %, 1.5 %, 0.8 %, and 0.0006 %, respectively table (6).

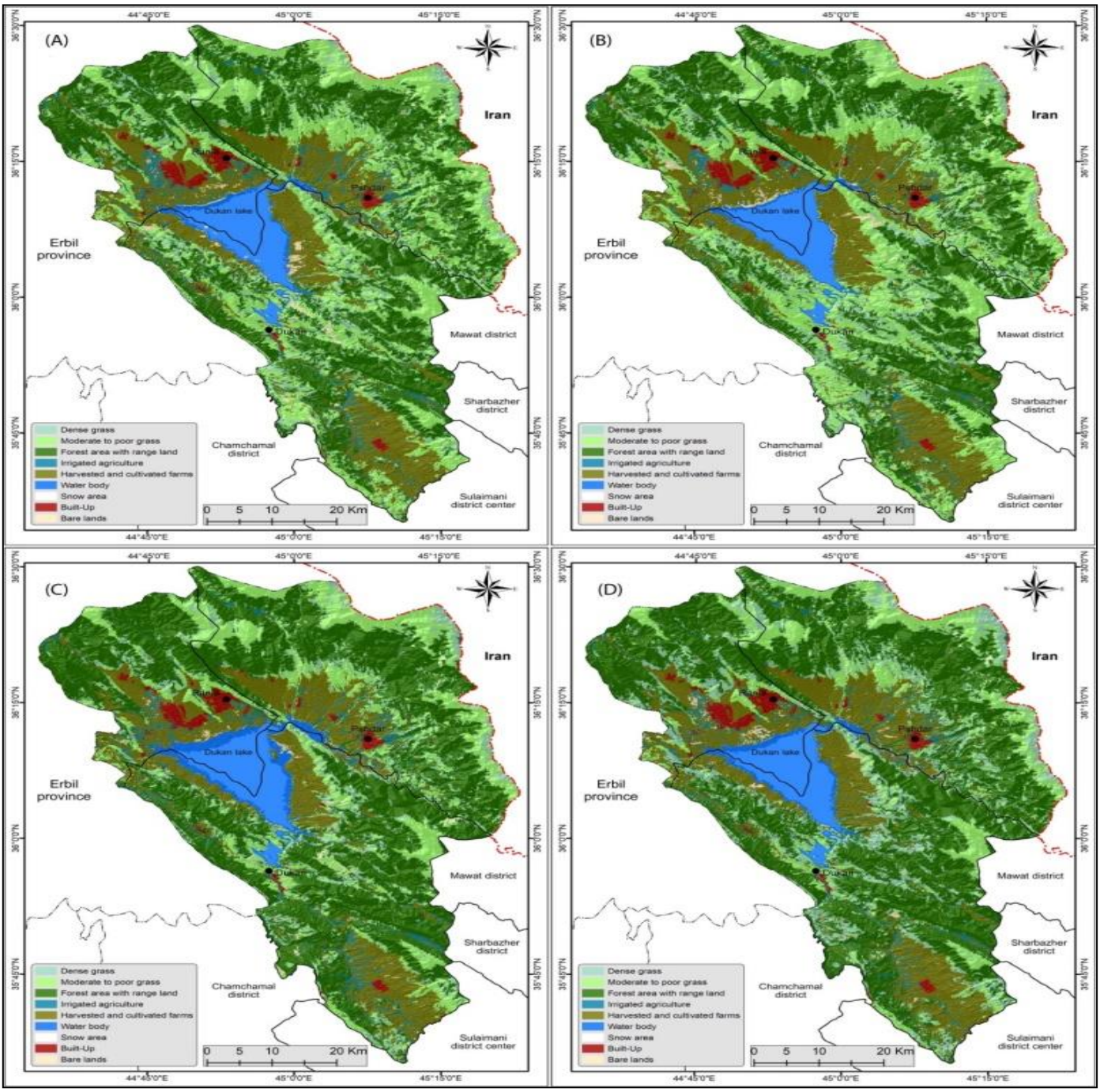

Figure (6); OBI classification results: A) 2017, B) 2018, C) 2019, and D) 2020

Table (7) summarizes the detail of the LULC change area (gains and losses) from 2013 to 2020. Throughout the study phases, the LULC categories area rate grows and decreases in an unstable manner, with the exception of the Built – Up area, which increases steadily from the first to the final phase of the study periods. In general, from the beginning to the end of the phase, each category of bare lands, built-up land, irrigated agriculture, and forest area with range land gains at a rate of (96.34%, 34.16%, 26.6%, and25.42%) respectively. During the same time period, each category of snow area, moderate to poor grass, dense grass, harvested and cultivated farms, and water body lost their area by (93.5%, 22.3%, 7.23%, 3.84%, and 2.58%). Table (7) and figure (8).

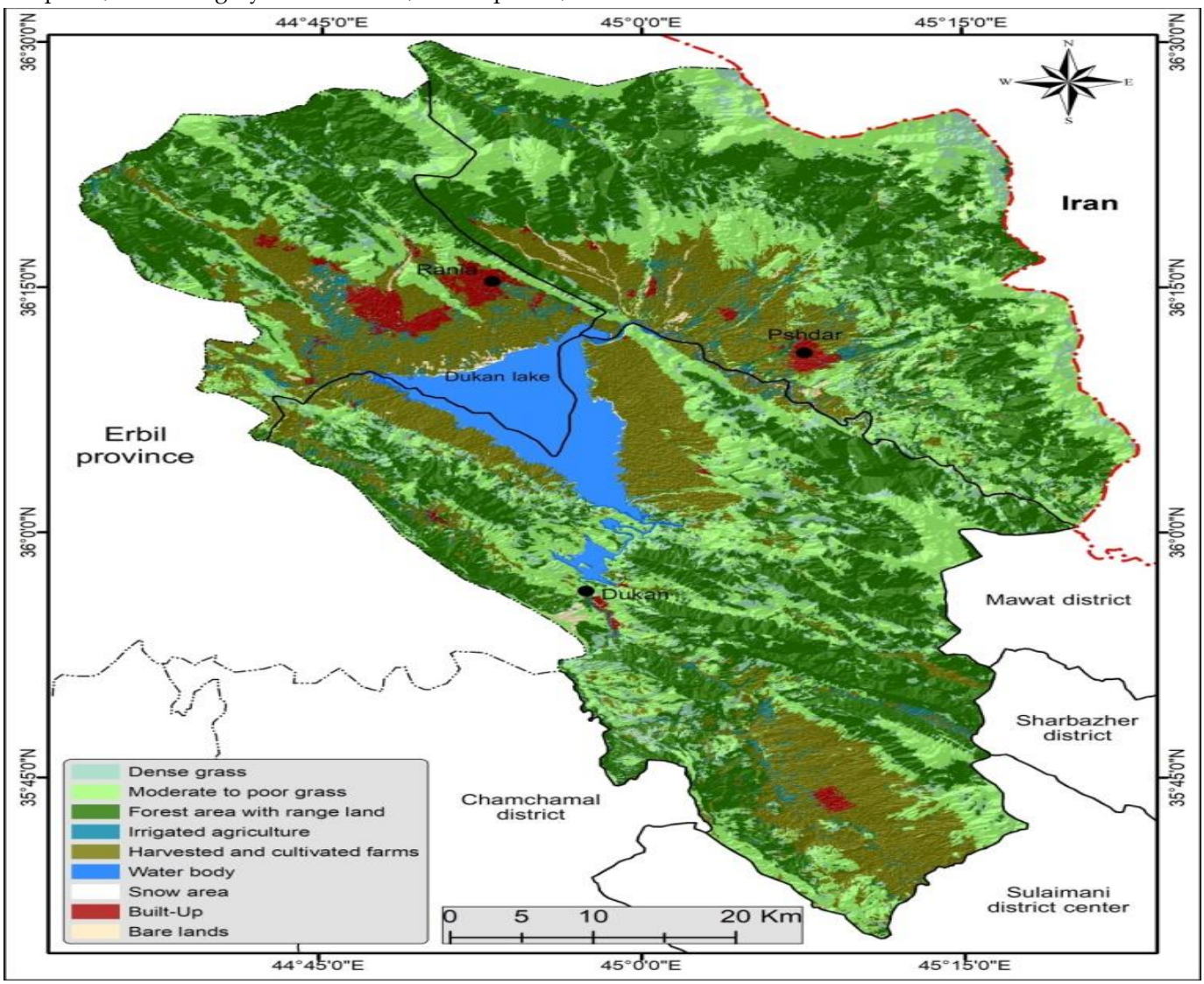

Figure (7); OBI classification results for the last stage of study periods (2021)

Table (6); LULC classification results for 2013 to 20121 images showing the area of each category and category percentages in (northern of Sulaimani province)

LULC class	2013		2014		2015		2016		2017		2018		2019		2020		2021	
	KM²	%	KM²	%	KM²	%	KM²	%	KM²	%	KM²	%	KM²	%	KM²	%	KM²	%
dense grass	369.64	9.21	424.3	10.6	428.3	10.7	418	10.4	366	9.13	383	9.6	335	8.3	534	13.3	343	8.5
moderate to poor grass	1287.6	32.1	1283	32	1126	28.1	836	20.8	987	24.6	1096	27	649.5	16	495	12.3	1001	25
forest Area with range land	1193	29.7	1119	27.9	1261	31.4	1583	39.4	1477	36.8	1360	34	1842	46	1808	45.1	1496	37
irrigated agriculture	60.812	1.52	71.88	1.79	69.34	1.73	99.3	2.48	106	2.65	77.8	1.9	113.2	2.8	93.4	2.33	77	1.9
harvested and cultivated farms	854	21.3	870.9	21.7	869.9	21.7	753	18.8	758	18.9	792	20	717.5	18	759	18.9	821	20
water body	184.93	4.61	157.3	3.92	153.7	3.83	242	6.03	214	5.33	202	5	261.6	6.5	227	5.65	180	4.5
snow area	0.3557	0.01	0.293	0.01	0.18	0	0.02	0	0.01	0	0	0	0.041	0	0.03	0	0.02	0
Built-Up	45.855	1.14	48.96	1.22	50.27	1.25	52	1.3	54.3	1.35	55.6	1.4	57.12	1.4	59.5	1.48	61.5	1.5
bare lands	16.7	0.42	37.76	0.94	54.55	1.36	30.6	0.76	49.8	1.24	46.5	1.2	36.99	0.9	37.6	0.94	32.8	0.8
Total	4012.9	100	4013	100	4013	100	4013	100	4013	100	4013	100	4013	100	4013	100	4013	100

Table (7) LULC classification results from 2013 to 20121Image depicting area change (loss or gain) and percentage in (north of Sulaymaniyah governorate)

LULC class	2013-2014		2014-2015		2015-2016		2016-2017		2017-2018		2018-2019		2019-2020		2020-2021		2013-2021	
	KM²	%	KM²	%	KM²	%	KM²	%	KM²	%	KM²	%	KM²	%	KM²	%	KM²	%
dense grass	54.6	14.8	4.04	0.95	-11	-2.52	-51.1	-12.2	17	4.65	-48.5	-13	198.6	59.3	-191	-35.7	-27	-7.23
moderate to poor grass	-5.1	-0.4	-157	-12	-290	-25.8	151.2	18.1	109	11.1	-447	-41	-154	-24	506	102	-287	-22.3
forest area with range land	-74	-6.2	142	12.7	322	25.54	-106	-6.7	-117	-7.9	482	35.4	-34	-1.8	-312	-17.2	303	25.42
irrigated agriculture	11.1	18.2	-2.5	-3.5	30	43.27	6.89	6.94	-28.4	-27	35.37	45.5	-19.7	-17	-16.4	-17.6	16.2	26.6
harvested and cultivated farms	16.9	1.98	-1	-0.1	-117	-13.5	5.222	0.69	33.5	4.42	-74.2	-9.4	41.45	5.78	62.3	8.21	-33	-3.84
water body	-28	-15	-3.7	-2.3	88.1	57.35	-27.7	-11.5	-12.2	-5.7	59.75	29.6	-35	-13	-46.4	-20.5	-4.8	-2.58
snow area	-0.1	-18	-0.1	-38	-0.2	-86.8	-0.01	-38.7	-0.01	-97	0.041	9050	-0.02	-38	-0	-10.5	-0.3	-93.5
Built-Up	3.11	6.78	1.31	2.67	1.74	3.465	2.303	4.43	1.33	2.44	1.479	2.66	2.352	4.12	2.05	3.44	15.7	34.16
bare lands	21.1	126	16.8	44.4	-24	-43.9	19.25	62.9	-3.36	-6.7	-9.5	-20	0.646	1.75	-4.84	-12.9	16.1	96.36

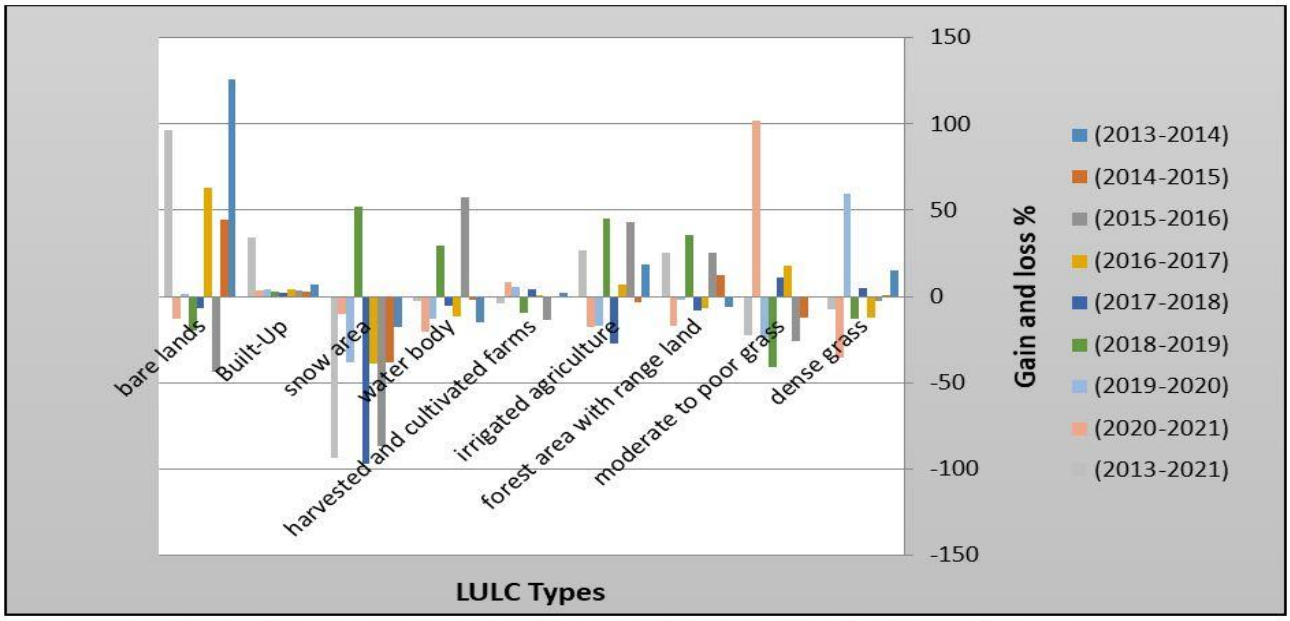

Figure (8); LULC change area (Gain and loss) with (%) during the study phases

4-3 Accuracy Assessment:

Table (8) summarizes the object-based image classification accuracy discovered throughout the accuracy assessment process for the time period frames (2013-2021). The LULC classification levels' overall accuracy ranged from 91.7 to 92.35 percent, with Kappa coefficients of agreement ranging from 0.906 to 0.9137. The accuracy of each LULC class (user accuracy (UA) and producer accuracy (PA)) is shown in same table. According to (Feizizadeh. B, et al., 2021) classification Accuracy scheme, these values of Accuracy Assessment for all classification stages findings for the study area are Very High Confidence in Classification (VHCC), because they are more than 90% accurate.

Table (8): Accuracy assessment result for the nine phase LULC maps in the study area

LULC Class	2013		2014		2015		2016		2017		2018		2019		2020		2021	
	PA	UA	PA	UA	PA	UA	PA	UA	PA	UA	PA	UA	PA	UA	PA	UA	PA	UA
dense grass	89.79	92.36	89.5	92.1	89.6	92.3	89.7	92.29	89.8	92.3	89.9	92.4	89.9	92.5	89.9	92.5	90.1	92.6
moderate to poor grass	91.75	90.63	91.9	90.8	92	90.9	91.97	90.87	92	91	92.1	91	92.1	91	92.2	91.1	92.3	91.3
forest area with range land	89.44	90.31	89.3	90.2	89.3	90.2	89.44	90.31	89.4	90.3	89.5	90.4	89.7	90.5	89.7	90.5	89.7	90.5
irrigated agriculture	93.7	90.31	93.7	90.3	93.7	90.3	93.77	90.42	93.8	90.5	93.9	90.7	94	90.8	94	90.7	94.1	90.9
harvested ad cultivated farms	92.01	90.69	92.2	90.9	92.2	91	92.2	90.91	92.2	91	92.3	91.1	92.4	91.2	92.5	91.2	92.7	91.5
water body	95.89	97.36	96.3	97.6	96.3	97.6	96.27	97.61	96.3	97.6	96.3	97.6	96.3	97.6	96.3	97.6	96.3	97.6
snow area	89.51	91.62	89.8	91.9	90.1	92.1	90.05	92.06	90	92	90.1	92.1	90.2	92.2	90.1	92.1	90.3	92.3
Built-up	90.91	86.96	92	88.5	91.4	87.6	91.75	88.12	92.5	89.2	92.9	89.7	93.2	90.1	93.3	90.3	93.5	90.6
bare lands	89.84	90.91	89.7	90.8	89.9	90.9	90.23	91.25	90.2	91.3	90.4	91.4	90.6	91.6	90.8	91.8	91.2	92.1
Over All Accuracy	91.7		91.9		91.94		92		92.03		92.12		92.2		92.24		92.35	
Kappa Coefficient	0.906		0.908		0.909		0.9093		0.9099		0.911		0.912		0.9123		0.9137	

4-4 determining the impact of annual average change of climate elements on LULC change

According to the discussion in the preceding paragraphs, there have been numerous variations in LULC as well as annual changes in climate factors across the study period. Looking at the data above, it's evident that there's a strong correlation between changes in LULC and changes in the average yearly climate in general. Annual variations in climate components, on the other hand, have had an impact on land cover shifts (water bodies, general surface vegetation, snow cover, and bare lands). As shown in figure (9), during the study period of 2013 to 2021, variations in the distribution of rainfall average and relative humidity were detected, while the area of water bodies, thick grass, and forest area mixed with dense grass fluctuated in the same direction. At the same time, the average rainfall and humidity, as well as the change in bare lands and the moderate to poor grass area, all point in the opposite direction. Although the average temperature has direct and indirect effects on all LULC types, the impact of these climate components is more obvious than the change in the snow area in the highlands, particularly the temperature change between the end of the spring season and the start of the summer season. On the other hand, it is either relevant or very weak in terms of the association between average yearly changes in climatic components and other land uses, particularly Built-Up. Regarding to Agricultural land uses (irrigated agriculture, harvested and cultivated farms) had very little impact during the study period, despite the fact that these climate characteristics are the most important factor in agricultural products. This is because the study area's major agricultural irrigation system was based on irrigated rain fodder, and the study area picked the rainfall area Confirmed in terms of agricultural production system at the same time and contains a variety of water sources as well.

We return to Tables (3, 4, 5, 6, and 7) to further clarify the relationship between LULC change and annual changes in climate components in the study area. As it is shown year (2019) had the highest rainfall (1038 mm) and humidity (50.03 %), as well as the lowest temperature (19.8°). Simultaneously, the

area of snow, irrigated agriculture, forest area with range land, and water body classes have increased by a range of 278.4 %, 45.5 %, 35.4 %, and 29.6 %, respectively, while the area of moderate to poor grass, bare lands, dense grass*, and harvested and cultivated farms has decreased by a range of (41 %, %, 13 %, and 9.4 %) compared to the previous stage. In contrast, the area of dense grass, water body, irrigated agriculture, forest area with range land, and snow classes have decreased by a range of 35.7 %, 20.5 %, 17.6 %, 17.2 %, and 10.5 %, respectively, while the area of moderate to poor grass, harvested and cultivated farms have expanded by a variety of rates (102%, and 8.21%) at the end of the study phase in 2021, which recorded the lowest rainfall (351.6mm) and humidity (39.99 %), as well as the highest temperature (21.88 °). This demonstrates that annual average climatic change has had a significant impact on LULC change in northern Sulaymaniyah during the research period, as well as it confirms the effective of the mythology.

5- Conclusion and Prospects:

Land use and land cover change, as well as climate change and its consequences, are considered to be among the most pressing global, regional, and local concerns. Countries, academic institutions, and organizations involved in this subject, as well as academics, have made constant efforts in the past to determine the causes and consequences of these two issues. Although there are many and various reasons of change in LULC and climate change, each of them is a cause of change in the other, implying a bilateral relationship, or an exchange. In this study, statistical data and image satellite data were combined, and we developed a new and more efficient methodology based on the annual average of climate elements, OBIA methods, and several other new and more effective techniques, with the goal of detecting LULC changes over the last nine years (2013-2021), as well as identifying and analyzing the effect of the annual average change of climate elements on LULC changes. The accuracy evaluation results of this investigation, on the other hand, demonstrate the efficacy of the study approach and corroborate our findings. Finally, the findings demonstrate that there has been a considerable shift in the composition of the climate, coinciding with the LULC, during the various stages of the study, indicating that climate change has had a significant impact on LULC change in the studied area, although the impact differed from one LULC type to another from one year to the next. Despite this, we must be aware that LULC changes are not solely due to climate change. However, various additional factors such as (population, city expansion, grassland burning, and natural resource management styles...etc.) have influenced the change in LULC during the study period in the study area. Finally, we believe that the findings of this effort will aid governmental institutions and experts in formulating the optimal strategy for the LULC's future direction and better anticipating future environmental problems.

(*) The decrease in the area of dense grass in 2019 is due to the large number of fires that occurred in the study area especially in the rangeland of Qandil, Asos, and Qarasird area as we noted during the satellite imagery.

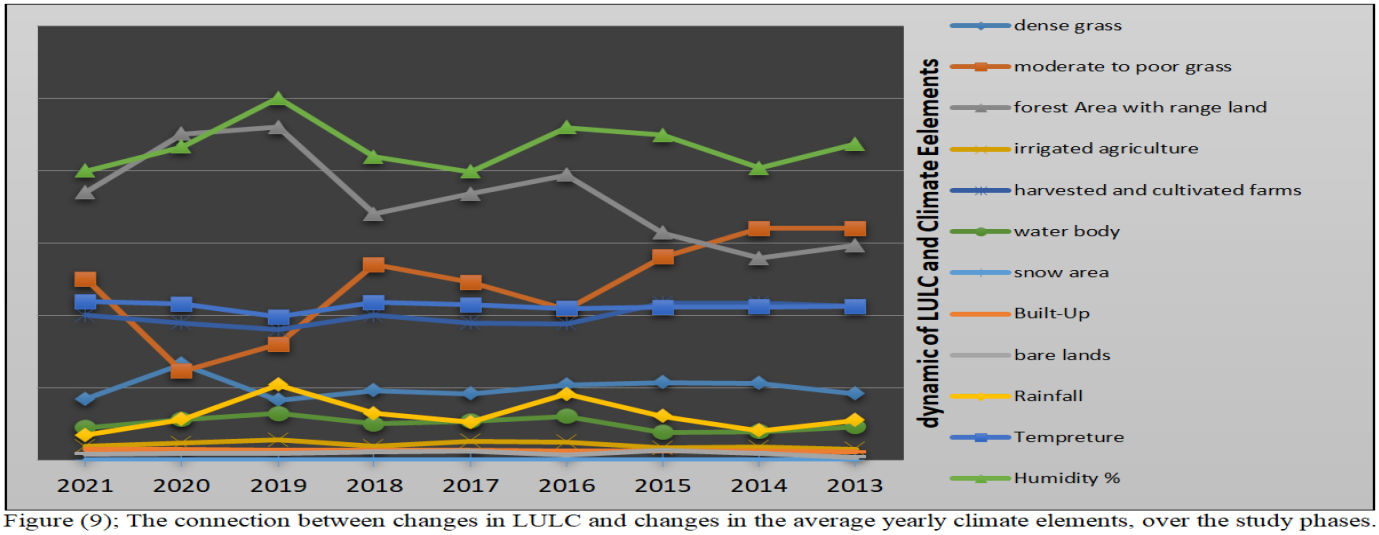

Figure (9): The connection between changes in LULC and changes in the average yearly climate elements, over the study phases.

6- References:

Aggarwal, S. P., Garg, V., Gupta, P. K., Nikam, B. R., & Thakur, P. K. (2012). Climate and LULC change scenarios to study its impact on hydrological regime. International Archives of the Photogrammetry, Remote Sensing and Spatial Information Sciences, 39(B8), 147-152.

Ali, M. I., Dirawan, G. D., Hasim, A. H., &Abidin, M. R. (2019). Detection of changes in surface water bodies urban area with NDWI and MNDWI methods. International Journal On Advanced Science Engineering Information Technology, 9(3), 946-951.

Bhatti, S. S., &Tripathi, N. K. (2014). Built-up area extraction using Landsat 8 OLI imagery. GIScience& remote sensing, 51(4), 445-467.

Chen, H., Zhang, W., Gao, H., &Nie, N. (2018). Climate change and anthropogenic impacts on wetland and agriculture in the Songnen and Sanjiang Plain, Northeast China. Remote Sensing, 10(3), 356.

Dale, V. H. (1997). The relationship between land-use change and climate change. Ecological applications, 7(3), 753-769.

DeWitt, J. D., Chirico, P. G., Bergstresser, S. E., & Warner, T. A. (2017). Multi-scale 46-year remote sensing change detection of diamond mining and land cover in a conflict and post-conflict setting. Remote Sensing Applications: Society and Environment, 8, 126-139.

Dharani, M., &Sreenivasulu, G. (2021). Land use and land cover change detection by using principal component analysis and morphological operations in remote sensing applications. International Journal of Computers and Applications, 43(5), 462-471.

Diener, B. J., & Frank, W. P. (2010). The China-India challenge: A comparison of causes and effects of global warming. International Business & Economics Research Journal (IBER), 9(3).

Dong, S., Chen, Z., Gao, B., Guo, H., Sun, D., & Pan, Y. (2020). Stratified even sampling method for accuracy assessment of land use/land cover classification: a case study of Beijing, China. International Journal of Remote Sensing, 41(16), 6427-6443.

Fasona, M. J., Soneye, A. S., Ogunkunle, O. J., Adeaga, O. A., Fashae, O. A., & Abbas, I. I. (2014). Simulating Land-Cover and Land-Use Change in the SavannaUnder Present Day and Future Climate Scenarios-A GIS-Based Approach. Earth Science Research, 3(1), 25.

Feizizadeh, B., MohammadzadeAlajujeh, K., Lakes, T., Blaschke, T., &Omarzadeh, D. (2021). A comparison of the integrated fuzzy object-based deep learning approach and three machine learning techniques for land use/cover change monitoring and environmental impacts assessment. GIScience& Remote Sensing, 1-28.

Feizizadeh, B., MohammadzadeAlajujeh, K., Lakes, T., Blaschke, T., &Omarzadeh, D. (2021). A comparison of the integrated fuzzy object-based deep learning

approach and three machine learning techniques for land use/cover change monitoring and environmental impacts assessment. GIScience& Remote Sensing, 1-28.

Georganos, S., Lennert, M., Grippa, T., Vanhuysse, S., Johnson, B., & Wolff, E. (2018). Normalization in Unsupervised Segmentation Parameter Optimization of Global Score: A solution based on Local Regression Trend Analysis. Remote Sensing, 10(2).

Goodin, D. G., Anibas, K. L., &Bezymennyi, M. (2015). Mapping land cover and land use from object-based classification: an example from a complex agricultural landscape. International Journal of Remote Sensing, 36(18), 4702-4723.

Hossen, S., Hossain, M. K., &Uddin, M. F. (2019). Land cover and land use change detection by using remote sensing and GIS in Himchari National Park (HNP), Cox's Bazar. Bangladesh. J. Sci. Technol. Environ. Inform, 7(02), 544-554.

Idowu, T. E., Waswa, R. M., Lasisi, K., Nyadawa, M., &Okumu, V. (2020). Object-based land use/land cover change detection of a coastal city using Multi-Source Imagery: a case study of Lagos, Nigeria. South African Journal of Geomatics, 9(2), 136-148.

Johnson, B. A., & Ma, L. (2020). Image segmentation and object-based image analysis for environmental monitoring: Recent areas of interest, researchers' views on the future priorities.

Lamichhane, S., &Shakya, N. M. (2019). Integrated assessment of climate change and land use change impacts on hydrology in the Kathmandu Valley watershed, Central Nepal. Water, 11(10), 2059.

Leary, N., Kulkarni, J., &Seipt, C. (2007). Assessment of Impacts and Adaptation to Climate Change: Final Report of the AIACC Project. In Assessment of Impacts and Adaptation to Climate Change: Final report of the AIACC Project (pp. 216-216).

Li, C., Li, Z., Yang, M., Ma, B., & Wang, B. (2021). Grid-Scale Impact of Climate Change and Human Influence on Soil Erosion within East African Highlands (Kagera Basin). International Journal of Environmental Research and Public Health, 18(5), 2775.

Lyons, M. B., Keith, D. A., Phinn, S. R., Mason, T. J., &Elith, J. (2018). A comparison of resampling methods for remote sensing classification and accuracy assessment. Remote Sensing of Environment, 208, 145-153.

Ma, L., Liu, Y., Zhang, X., Ye, Y., Yin, G., & Johnson, B. A. (2019). Deep learning in remote sensing applications: A meta-analysis and review. ISPRS journal of photogrammetry and remote sensing, 152, 166-177.

Ming, D., Li, J., Wang, J., & Zhang, M. (2015). Scale parameter selection by spatial statistics for GeOBIA: Using mean-shift based multi-scale segmentation as an example. ISPRS Journal of Photogrammetry and Remote Sensing, 106, 28-41.

Ministry of transport and communications, 2020, general directorate of meteorology and earthquake of Kurdistan region

Näschen, K., Diekkrüger, B., Evers, M., Höllermann, B., Steinbach, S., &Thonfeld, F. (2019). The impact of land use/land cover change (LULCC) on water resources in a tropical catchment in Tanzania under different climate change scenarios. Sustainability, 11(24), 7083.

Son, N. T., Chen, C. F., Chang, N. B., Chen, C. R., Chang, L. Y., &Thanh, B. X. (2014). Mangrove mapping and change detection in Ca Mau Peninsula, Vietnam, using Landsat data and object-based image analysis. IEEE Journal of Selected Topics in Applied Earth Observations and Remote Sensing, 8(2), 503-510.

Talukdar, S., Singha, P., Mahato, S., Pal, S., Liou, Y. A., &Rahman, A. (2020). Land-use land-cover classification by machine learning classifiers for satellite observations—a review. Remote Sensing, 12(7), 1135.

Thakur, T. K., Patel, D. K., Bijalwan, A., Dobriyal, M. J., Kumar, A., Thakur, A., ...&Bhat, J. A. (2020). Land use land cover change detection through geospatial analysis in an Indian Biosphere Reserve. Trees, Forests and People, 2, 100018.

Tian, J., & Chen, D. M. (2007). Optimization in multi-scale segmentation of high-resolution satellite images for artificial feature recognition. International Journal of Remote Sensing, 28(20), 4625-4644.

Twisa, S., &Buchroithner, M. F. (2019). Land-use and land-cover (LULC) change detection in Wami river basin, Tanzania. Land, 8(9), 136.

Venkataramanan, M. (2011). Causes and effects of global warming. Indian Journal of Science and Technology, 4(3), 226-229.

Vivekananda, G. N., Swathi, R., &Sujith, A. V. L. N. (2021). Multi-temporal image analysis for LULC classification and change detection. European journal of remote sensing, 54(sup2), 189-199.

Ye, S., Pontius Jr, R. G., &Rakshit, R. (2018). A review of accuracy assessment for object-based image analysis: From per-pixel to per-polygon approaches. ISPRS Journal of Photogrammetry and Remote Sensing, 141, 137-147.